Preparation and characterization of green adsorbent on functionalized and nonfunctionalized ALOE VERA: A combined experimental and DFT calculations

D. Ikhou, A. Guendouzi, M. Kaid, H. Ziani, Didier Villemin, A. Chakraborty

Preparation and characterization of green adsorbent on functionalized and non-functionalized ALOE VERA: A combined experimental and DFT calculations

D. Ikhou [a], A. Guendouzi [b,*], M. Kaid [a], H. Ziani [a], D. Villemin [c], A. Chakraborty [d]

[a] *Laboratory of Physico-chemical Studies, Department of Physics, Faculty of Sciences, University of Saïda, Algeria*

[b] *Laboratory of Chemistry, Synthesis, Properties and Applications, Department of Chemistry, Faculty of Sciences, University of Saïda, Algeria*

[c] *LCMT, ENSICAEN, UMR 6507 CNRS, National School of Engineering and Research Center, University of Caen, 6 bd Ml Juin, Caen, 14050, France*

[d] *Department of Physics, The University of Burdwan, Golapbag Campus, Burdwan, 713104, West Bengal, India*

ARTICLE INFO

Keywords:
Aloe Vera (AV)
Adsorption process
Lead and cadmium DFT calculations

ABSTRACT

An influential subject of research is the preparation of raw Aloe-Vera (AV) which is characterized by FTIR, XRD, SEM, and BET and its use as a biosorbent for the effective removal of Pb(II) and Cd(II) ions from an aqueous solution. The adsorption study was studied using UV–visible (UV/Vis) spectroscopy. The adsorption capacity of Pb(II) by AV is 36.33 mg/g (95,79%) was obtained at 20 min at acidic pH = 3, whereas the optimal sorption of Cd(II) is 16.92 mg/g (81.54%) at 15 min at pH = 6 with a mass of adsorbent of 0.05 g and metal ion concentration of 5.10–4 M at 20 °C. Thermodynamic studies have proven that the removal of Pb (II) and Cd (II) using AV is spontaneous, endothermic, and physical in nature. The adsorption kinetics follows the pseudo-second-order process and the isotherm adsorption was most accurately described by the Freundlich model. On the other hand, based on the enormous power of the density functional theory as a tool in the adsorption phenomena, which has been greatly improved by their applications to organic and inorganic adsorption design. The functionalB97D3 with 6-311++G**/land2dz//SMD basis set and solvent model is used using descriptors as molecular, electronic, and reactivity indices.

1. Introduction

Pollution of the biosphere by toxic metals has accelerated dramatically due to the explosive growth of the industry. The presence of various heavy metals in aqueous effluents is harmful to human health and the environment [1–3]. Among these significant metals, lead and cadmium are believed to be highly dangerous and carcinogenic, even at low concentrations, which have a negative influence on many biological processes and environmental [4]. These metals are generally non-biodegradable, extremely toxic, and carcinogenic to the health and the environment if they are not removed from wastewater before it is released into the environment.

Cadmium is a well-known toxic and persistent pollutant that occurs naturally at very low concentrations in common aquatic environments [5]. Cd (II) is also used in many processes, such as batteries, plastics and pigments [6]. It can accumulate in several organs of the human body producing negative effects such as blood pressure and kidney complications [7] and has a carcinogenic effect [6,8]. Lead exists in industrial and agricultural wastewater; it is seriously dangerous for humans and living beings. Long-term drinking water containing a high level of Pb (II) would cause serious disorders, such as kidney disease, nausea, coma, seizures, cancer, as well as subtly negative effects on metabolism and intelligence [9]. Due to their hazardous effects on the environment and human health, it is important to develop a simple and sensitive analytical method in order to improve the quality of the environment and human life. Several industrial wastewater treatment methods for the removal of these cations have been reported in the literature [10].

The adsorption technology is one such method considered an attractive method, most popular for its efficiency in removing heavy metal ions from effluents in aqueous solutions [11,12]. It is a clean and fast operation, characterized by its ease of handling, its low cost, and the availability of different adsorbents in large quantities, easily regenerable and inexpensive. The economy of this method depends mainly on the

cost of the adsorbent materials and their availability in large and renewable quantities, efficiently, and inexpensively [13–16].

Many researchers are attempting to evaluate the sorption capacities of various new materials in order to research other economically and inexpensive adsorbents in huge quantities, such as natural materials at low-cost adsorbents and an effective adsorbent as hydroxyapatite for the removal of metal ions lead and cadmium from liquids solutions [17–21].

Aloe Vera leaves are easily found in many places in Algeria. It is a succulent plant, with a whorl of inexperienced elongated, pointed leaves which belongs to the Liliaceae family [12], it is found everywhere as a remarkable therapeutic plant with its various applications. Recently, many studies have reported the use of Aloe Vera as a biosorbent to eliminate Cu (II), Cr (III) [22–24], Zn (II) [25], As [26], Cr (VI) [27].

In the present work, we are interested in the preparation of the Aloe Vera (AV) leaves in the raw state as biosorbent and its application for the adsorption of Pb (II) and Cd (II) ions from aqueous solutions.

With this in mind, we carried out a parametric study of the adsorption phenomenon of these metallic ions by examining the various parameters effects like contact time, adsorbent mass, pH solution, temperature, and the effect of ionic strength.

2. Materials and methods

2.1. Material

The Aloe Vera (AV) leaves were collected in the Saïda region in Algeria. Stock solutions of lead (II) and cadmium (II) were prepared by dissolving lead acetate $PbC_4H_6O_4.3H_2O$ (99.8%, Riedel De Haen), cadmium acetate Cd $(CH_3COO).2H_2O$ (99%, Prolabo) in distilled water (DW).). A buffer solution of CH_3COOH/CH_3COONa (99% Riedel De Haen) was prepared to keep the pH constant during Pb (II) and Cd (II) spectrophotometer analysis with Xylenol orange $C_{31}H_{28}N_2Na_4O_{13}S$ (99% Aldrich), the pH of the solution was adjusted to the desired value by dropwise addition of 0.1 M CH_3COOH (98% Panreac) using a digital pH meter of the consort C863 type. Distilled water was used. All other reagents were analytical reagent grade.

2.2. Preparation of Aloe vera biosorbent

The sample from (AV) was washed with a mixture of ethanol and acetone two to three times to remove chlorophyll (green color of the plant), followed by several washes with distilled water to remove dust and other unwanted impurities. Then, it was dried in an oven at 80 °C for 24 h, and ground using a standard sieve to separate the powder by 0.2–0.3 μm the obtained materials were stored until the time of use in adsorption experiments.

2.3. Characterization of adsorbent

In order to study the mechanism of adsorption of metals, it is important to determine the chemical composition of the materials obtained as well as their surface morphology. Infrared spectroscopy was performed by the Fourier transform infrared spectrometer type SHIMADZU FTRI 8400, in the range (4000–400 cm^{-1}). Scanning electron microscopy (SEM), used to examine the morphological structure of WAV and visualize its surface morphology, was performed on a JEOL-JSM-F100 microscope.

The X-ray diffraction patterns (XRD) of the samples were carried out on a diffractometer of the "Expert Prof Panalytical, type MPD and vertical system θ-θ" type, using Cu Kα radiation (λ = 0.15406 Å), a PDS pass (slit divergence program, slit Antiscater program).

2.4. Adsorption procedure

In order to determine the maximum adsorption yield and equilibrium data in this work, several adsorption experiments were investigated using aqueous solutions of Pb (II) and Cd (II). A stock solution of the metals at a concentration of 10^{-2} M was prepared in distilled water. From this stock solution, different concentrations were prepared by dilution. The adsorption study was carried out by adding 0.1 g of adsorbent to 10 mL of each metal solution (5.10^{-4} M) at the initial pH and at an ambient temperature of 20 ± 1 °C for a different time over a thermostatic stirrer with a stirring speed of 600 rpm. The adsorption studies were performed at 5–60 min.

The supernatant of the samples was centrifuged and analyzed by Double beam UV-VIS OPTEZEN 3220 for absorbance measurements at max = 585 nm, λ_{max} = 575 nm of Pb (II), and Cd (II) respectively with orange xylenol (colored indicators) to buffer 5.8 [28].

The amount (mg) of metal adsorbed per gram of adsorbent at the time (qt), adsorption capacity (mg g-1) at equilibrium (qe), and % removal were calculated using the following equations:

$$Removal\ \% = \frac{(Co - Ce).V.M}{m} \quad (1)$$

$$qe(mg/g) = \frac{(Co - Ce).V.M}{m} \quad (2)$$

$$qt(mg/g) = \frac{(Co - Ct).V.M}{m} \quad (3)$$

where $\mathbf{C_0}$ and **Ce** are the initial and equilibrium concentrations of Pb(II) and Cd(II) (mg L^{-1}); **m** is the amount of WAV (g) and **V**is the volume of the solution (L).

2.5. Theoretical study

In the present section, we review computational chemistry approaches used to investigate non-covalent interactions, from weak hydrogen bonds to metal-ligand interactions, using the DFT calculations.

2.5.1. Quantum chemical calculations

Density Functional Theory (DFT) [29,30] has been shown to be an adopted and useful tool for predicting and describing the chemical behavior of adsorption phenomena [31,32]. At the first, the initial structures of (AV@Pb//Cd) complex were generated by using Gaussview software [33],All DFT calculations of the optimization geometries, frontier molecular orbital analysisand harmonic vibrational frequencies were performed using the quantum chemistry packages ORCA [34].

B97-D3 exchange correlation functionals (including the D3 dispersion corrections) with extended basis sets6-311++G** [35] and a LANL2DZ [36] base set (for Pb and Cd atoms)were applied to optimize the standard structures with convergence criteria tightened without any geometric or symmetry constraints, thecomplexes obtained were verified using harmonic vibrational frequency calculations (the fact that all frequencies are real is a very important feature). In order to improve the accuracy of calculationsand to be as consistent as possible with the experimental environment, the effect of the solvent environment has been widely studied using the SMD model (Solvation Model based on Density) [37].

The second part of the theoretical framework is the calculation of the Fukui functions and the reactivity descriptors. According tothe purview conceptual density functional theory, frontier molecular orbitals (HOMO and LUMO) play a crucial role in determining which reactive sites have electrophilic or nucleophilic characteristics that explain the formation of H-bonds in the complex [38].

Finally, the analysis of atomic electronic populations on the k atom was calculated in anionic, neutral and cationic form, to give the information necessary for the evaluation of the Fukui indices f (r), using the following equations.

$$f_k^+ = [q_k(N+1) - q_k(N)]$$
$$f_k^- = [q_k(N) - q_k(N-1)]$$

where q_k(N-1), q_k (N) and q_k (N+1) represent the charge in site k in the three anionic, neutral and cationic systems, respectively.

3. Results and discussion

3.1. Characterization of the adsorbent

FTIR spectroscopy allows the identification of the functional groups present on the surface of the adsorbent; the AV spectrum is shown in Fig. 1. The strong absorption band is observed at 3419 cm-1, this may be due to the presence of hydrogen-bonded N–H stretching, characteristic of amino acids, and to the presence of –OH. The intense band at 2923 cm-1 is related to the symmetric and asymmetric C–H stretch of -CH2 groups, and the presence of aliphatic groups (-CH) is also indicated.

The other band shown in 1739 cm-1 is represented by the C=O stretch and the presence of carbonyl groups. The peak at 1547 cm-1 may be attributed to the aromatic nitro group (C–NO_2). FTIR peaks are shown on the surface of the AV adsorbent (1384 cm-1), (1384 -1060 cm-1), and (870 cm-1) indicating the presence of–COO^-, C – O – C, and C–H plane deformation of carbohydrate monomers Fig. 1.

The absorption bands at 870-631 cm-1 are related to the C–H out-of-plane of carbohydrate monomers. These results are in agreement with previous work [39,40].

Analysis of the FTIR spectra has also shown the presence of other ionizable functional groups (OH, CO, C = O, and C≡N) which can interact with cations [41–45]. This implies that these functional groups would remove the positively charged ions from the aqueous solution.

The X-ray diffraction (XRD) technique allows phase identification of a crystal structure and estimation of crystallite size. The XRD measurements were shown in Fig. 2, which has an amorphous structure and low crystallinity of the samples in the ranges of 14–25°. Two relatively broad peaks were observed in the AV powder at 2Θ = 14.95 and 2Θ = 21.7° diffraction on the (101) and (002) planes of the AV powder respectively [46].

The micrograph shows the presence of surface holes that correspond to the pores present in the material. These pores are responsible for the adsorption of the metal Fig. 3. These images revealed a porous and irregular surface (different heterogeneous surface structures) with deep pores such as granules, nanofibers, nanotubes, nanospheres, microspheres, and flakes [47] and aggregation of irregularly shaped grains, well interconnected that appear brighter, and flakes like a flat surface revealed [48–50].

The specific surface area of Aloe Vera was determined by the diode value method, the methylene blue value, and the Langmuir specific surface method [51]. The values of these methods realized from this sample are provided in Table 1.

The obtained results given in Table 1 indicate that the index value shows that the aloe vera adsorbent has a high microporosity and the

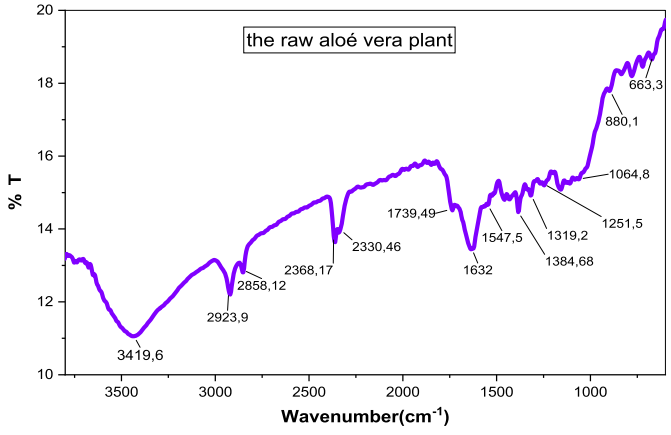

Fig. 1. FTIR spectra for Raw Aloe Vera powder.

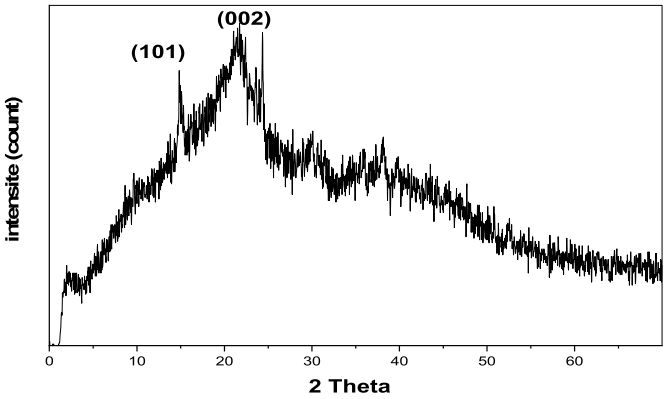

Fig. 2. XRD pattern of Raw Aloe vera powder.

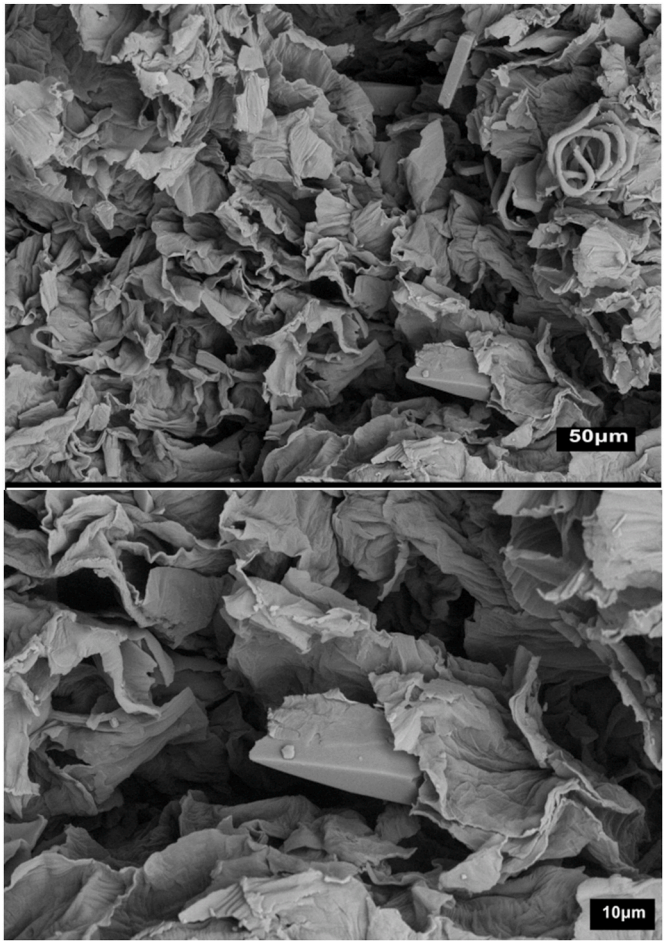

Fig. 3. SEM image of AV **(a)** at 50 µm and **(b)** 10 µm.

Table 1
Iodine value, methylene blue value, and Langmuir specific surface method.

Adsorbent	Iodine value (mg/g)	BM value (mg/g)	Specific area S_L (m^2/g)
Raw Aloé vera	361.68	4.02	13.84

result found by the methylene blue value indicates the porous quality of our material is of mesoporous types.

The Langmuir surface area value found in the present study (Table 1) is 13.84 m^2/g, which is nearly similar to the value of 14.62 m^2/g found by Gupta et al. [52].

3.2. Analysis of the influencing factors of adsorption experiments

3.2.1. The effect of contact time

The effect of contact time on the adsorption of Pb (II) and Cd (II) using AV was obtained in Fig. 4(a). The adsorption efficiency of the two metals on the adsorbent increases with increasing the contact time to certain limits to achieve a maximum sorption percentage of 87% and 80% at 20 min for Pb (II) and 15 min for Cd (II) respectively.

The rapid adsorption observed in the first step of this process may be because a large number of surfaces are available for adsorption and the formation of stable complexes between metal ions with the active site of the AV surface, which indicates a high affinity of this material for the two cations. In addition, the aggregation of these metals in the pores of the active sites begins to show resistance to the diffusion of heavy metal ions accumulated in the adsorbents [50,53]. After some time, it is observed that the adsorption yield decreases with increasing contact time, which is explained by the possibility of desorption of these ions due to weak adsorption bonds (van der Waals binding) and that the adsorption process proceeds according to physical adsorption; this means that the adsorption sites have reached equilibrium at the surface of the adsorbent.

3.2.2. The effect of the initial concentration

The effect of the initial concentration in an aqueous solution was studied at different concentrations of metal ions (10^{-3}, 2.10^{-4}, 5.10^{-4}, and 10^{-4} M) and the initial pH. The mixtures are followed for a different

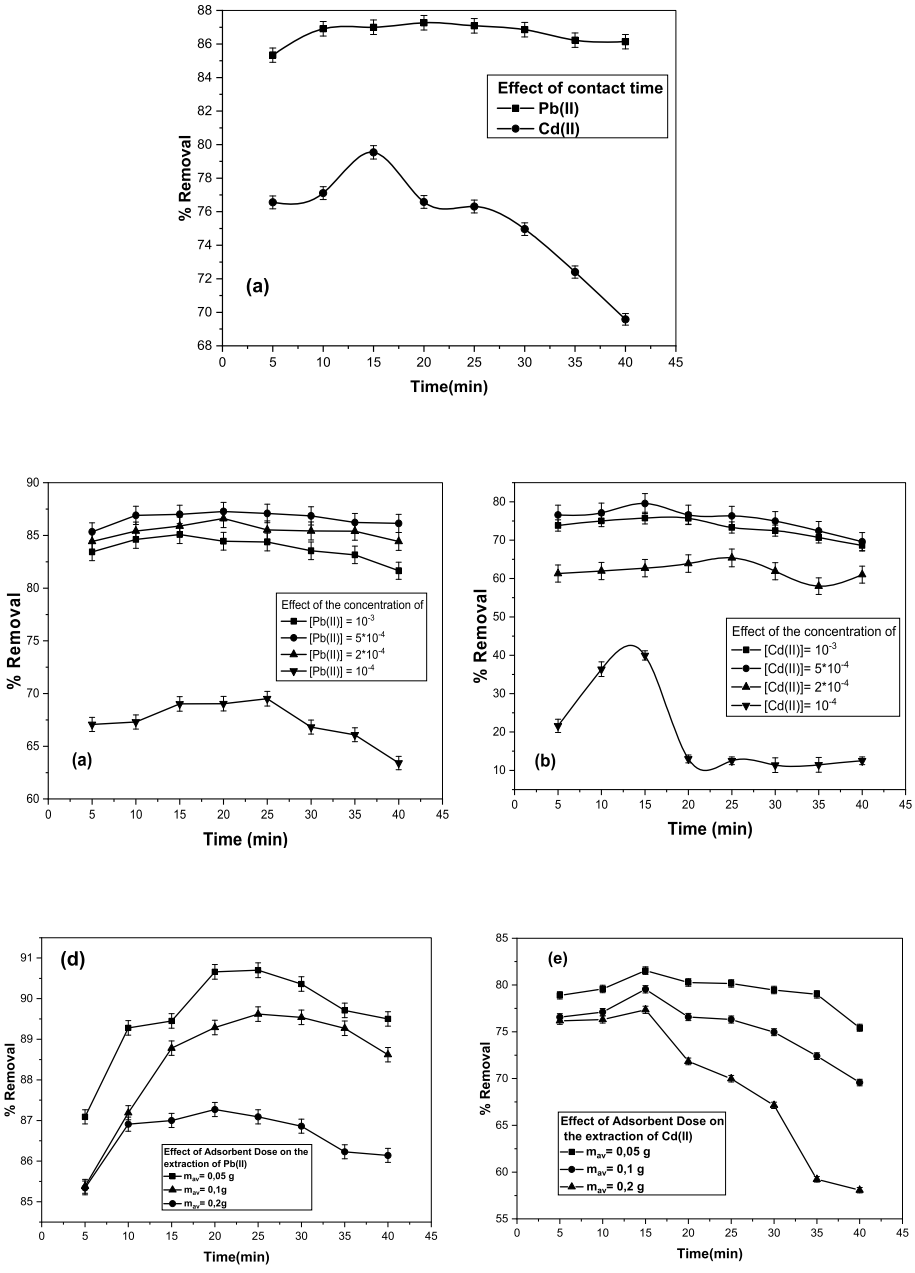

Fig. 4. Effect of different parameters: Contact time **(a).**Concentration effect **(c,d).**effect of Adsorbent dose effect **(d,e)** on the removal of Pb(II) and Cd(II) respectively.

period of time, as can be seen in Fig. 4 (b) and 4(c).

It has been shown that with a concentration of 5.10^{-4} M, the retention of the two cations reaches the maximum of 87% and 79% for Pb (II) and Cd (II) respectively. It is observed that at high concentrations (10^{-3}, 2.10^{-4} M) and at low concentrations (10^{-4} M), the yields are relatively reduced. This is probably due to the saturation of the adsorption sites of our material.

3.2.3. The effect of the adsorbent dose

The mass effect is an important factor in the adsorption process because it acts on the availability of active sites capable of fixing toxic heavy metals. It was studied by varying the adsorbent range from 0.05 to 0.2 g at a concentration of 5.10^{-4} M of aqueous solutions with initial pH at a temperature (20 °C), under a stirring speed of 600 rpm in the function of different times (Fig. 4d) and (Fig. 4e). This indicates that the adsorption of Pb (II) and Cd (II) on the adsorbent increases with time and reaches equilibrium at 20 min and 15 min respectively. The best yields were obtained with a mass of 0.05 g of AV adsorbent for the two cations reaching 91% Pb (II) and 82% Cd (II). Then, the adsorption decreased when the amount of adsorbent was increased from 0.1 to 0.2 g. Therefore, the amount of 0.05 g of adsorbent is sufficient to reach equilibrium. On the other hand, increasing the amount of AV decreases the adsorption of Pb and Cd. This can be explained by the following reasons [54]:

The total surface area of the adsorbent has decreased due to the aggregation of the adsorbent particles and the larger number of adsorbent leads to unsaturated adsorption sites.

3.2.4. The effect of pH

The pH of aqueous solutions is a critical parameter for the chelation and elimination of metals in the solid-liquid phase. The effect of pH was studied differently by adding acetic acid CH3COOH in aqueous solutions of metal ions. The results are shown in Fig. 6 (a) and 6(b).

To determine the species formed in our initial solutions of lead and cadmium used in the adsorption in aqueous medium at different pH values presented in Fig. 5, we undertook with the help of MEDUSA (Make Equilibrium Diagrams Using Sophisticated Algorithms) [55].

From Fig. 6(b), we notice that the yield or the sorption capacity of Cd (II) by AV increases rapidly in the pH range 3–6, it is (10.11–81,54%) or (2.11–16.92 mg/g). These results can be explained by the fact that acidity has a negative influence on the retention of Cd (II). The medium rich in H^+ and all the binding sites on the adsorbent undergo protonation and charge positively, which results in poor absorption due to

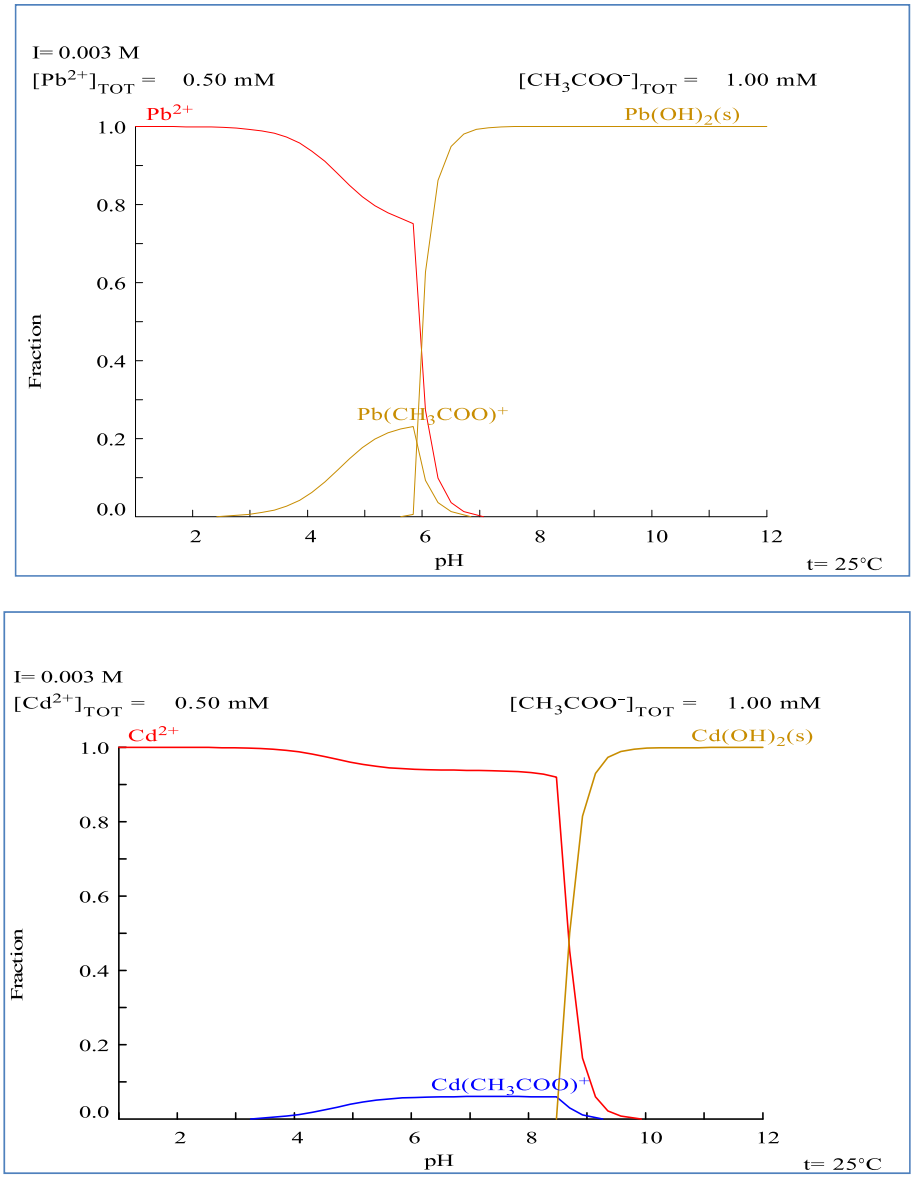

Fig. 5. Predominance diagram of Pb(II) and Cd(II) species in aqueous solution in acetate medium as a function of pH.

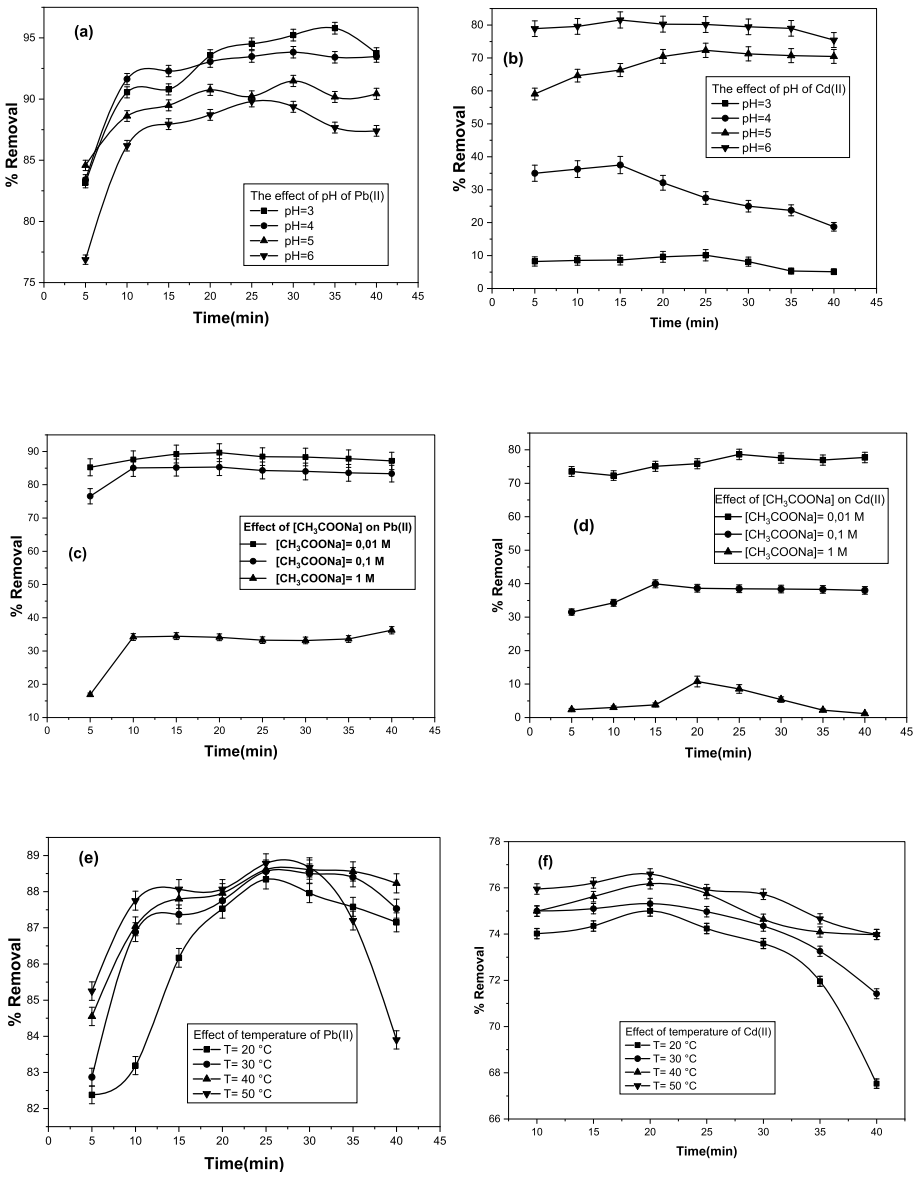

Fig. 6. Effect of pH **(a,b)**.Effect of CH_3COONa **(c,d)** and Temperature **(e,f)** on the removal of Pb(II) and Cd(II) respectively.

competition between Cd (II) ions and the sites of the adsorbent [56]. This can be explained by the fact that these ions form acetate complexes [57]. (See the species predominance diagram Fig. 5).

Whereas Pb (II) ions are preferred in an acidic medium which reaches an adsorption maximum of 95.79% (36.33 mg/g) at pH = 3 as shown in Fig. 6(a). The predominance diagram of the Pb (II) species Fig. 5 shows that the Pb (II) ions are free [58] and there is a formation of the acetate complex Pb $(CH3COO)^+$ in notable quantities, which is predominant in an acidic medium and are therefore likely to be adsorbed [59]. The pH effect has not been studied at higher pH values due to the presence of Pb $(OH)_2$ and Cd $(OH)_2$. The formation of these hydroxide species becomes important in reducing the adsorption of Pb (II) and Cd (II). Previous studies have also reported that the best adsorption efficiency of these ions was observed at pH [3–6,60].

3.2.5. *Effect of ionic strength*

The effect of ionic strength is one of the most influential parameters of adsorption. We have studied this phenomenon in order to know the competition between Na^+ and the cations of heavy metals studied. To determine this influence, three concentrations of CH3COONa (0.1, 0.01 and 0.5 M), were added to the aqueous phase of Pb (II) and Cd (II) at 5.10^{-4} M.

The results obtained are mentioned in Fig. 6(c) and (d), and we have shown that the more the concentration of CH_3COONa increases, the more the adsorption yield of the metal cations decreases and the best performances are obtained at low concentration of this salt to (0.01 M). As a result, high ionic strength can bring about a strong competition between the two cations and the sodium Na^+ ions generated by the dissolution of the salt, which forms a steric hindrance that led to a decrease in the adsorption yield on AV [61].

3.2.6. *Temperature effect*

The adsorption of Pb (II) and Cd (II) on the raw AV was studied as a function of temperature ranges 20–50 °C at the initial pH, with $[Pb^{+2}] = [Cd^{+2}] = 5.10^{-4}$ M and a mass of adsorbent equal to 0.05 g. The results are given in Fig. 6(e) and (f).

Temperature is a highly significant parameter in the adsorption process. The adsorption of Pb(II) ions increased from 73% to 76% and the removal of Cd(II) from 82% to 88% as the temperature increased from 20 to 50 °C, indicating that the process of Adsorption for both ions was endothermic, favored by an increase in temperature Fig. 6(e) and (f). The increase in the adsorption capacity of the AV adsorbent with

temperature can be attributed either to the increase in the number of active surface sites available on the surface of the adsorbent or by increasing the mobility of metal cations. Similar behavior in the removal of Pb (II) and Cd (II) was found using separate adsorbents [54,62–64].

3.3. Thermodynamic study

To determine the adsorption nature, the thermodynamic parameters including the change in the corresponding free energy (ΔG°), enthalpy (ΔH°), and entropy (ΔS°) were calculated from the following equations [57]:

$$\Delta G^\circ = \Delta H^\circ - T\Delta S^\circ \tag{4}$$

$$\ln \Delta G^\circ = -RT \ln K_d \tag{5}$$

$$\ln k_d = \frac{\Delta S^\circ}{R} - \frac{\Delta H^\circ}{RT} \tag{6}$$

The values of ΔH ° and ΔS ° can be determined from the slope and the intersection of a linear plot of ln Kdvs 1/T as shown in Fig. 7.

From the results of the thermodynamic study mentioned in Table 2, the negative values of the free energy ΔG ° are observed, which indicates that the nature of the phenomenon of adsorption of Pb (II) and Cd (II) ions on the AV is thermodynamically spontaneous, this indicates that there is a high-affinity for the adsorbed complex to penetrate the pores of this material [65,66]. However, the positive values of ΔH ° were respectively 1.912 and 0.706 kJ mol-1 for Cd (II) and Pb (II), showing that the process is endothermic.

Moreover, when ΔH <20 kJ mol-1, the adsorption process belongs to physical adsorption, while 80 kJ mol-1<ΔH <400 kJ mol-1. It belongs to chemical adsorption.

Therefore, the process of adsorption of two metals has physical adsorption. While the positive values of ΔS° suggest an increase in randomness and disorder at the solid/solution interface during the adsorption of Pb (II) and Cd (II) ions on the AV [54,65–67].

3.4. Adsorption isotherm

The adsorption isotherms have been developed to describe equilibrium relationships. It also explains the adsorption phenomenon is either physical or chemical [68]. In the present study, the Langmuir, Freundlich, Brunauer–Emmett–Teller (BET), D–R, and Temkin isotherms were applied to adjust the adsorption process of heavy metals. These models are represented in Fig. 8. And the experimental data at different parameters are in Table 3.

The Langmuir isotherm model has been based on the monolayer adsorption of metal ions adsorbate onto the adsorbent surface. The

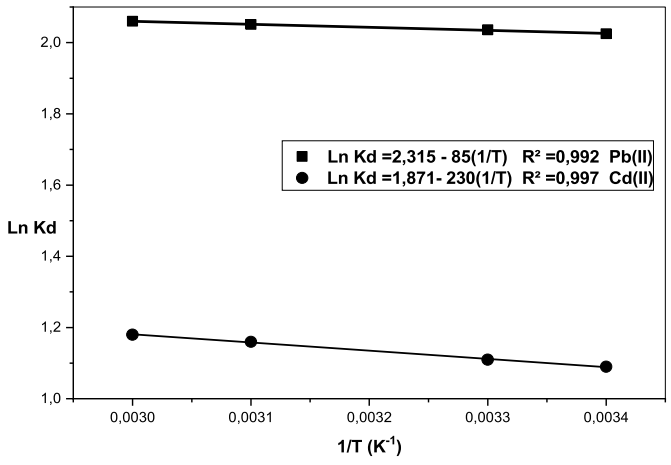

Fig. 7. Evolution of the Ln K_d in function of 1/T.

correlations used for predicting this model are [69]:

$$\frac{1}{q_e} = \frac{1}{K_L q_m C_e} + \frac{1}{q_m} \tag{7}$$

$$R_L = \frac{1}{1 + K_L C_e} \tag{8}$$

where **q_e:** is the amount of metal adsorbed per unit mass of biosorbent (mg/g), **Ce:** is the equilibrium concentration in solution (mg/L), and **K_L** and **q_m** are the adsorption capacity and rate of adsorption.

The Freundlich isotherm adsorption model discusses the type of adsorption on heterogeneous surfaces with interactions between adsorbed molecules [70]. The Freundlich formula is described by the following equation:

$$\text{Lg } q_e = \text{Lg } K_F + \frac{1}{n} \text{ lg } C_e \tag{9}$$

where **K_f** represents the Freundlich constant and **n** symbolizes the Freundlich factor (non-linear degree)

The Temkin model explains the influence of metal-metal interaction on the surface of the adsorbent. The model replies the heat of adsorption of all molecules in a layer as the function of temperature [71], which is expressed as:

$$q_e = B \ln A_T + B \ln C_e \tag{10}$$

$$\left(B_T = \frac{RT}{b_T}\right) \tag{11}$$

where **B**: is the Temkin constant, ***A_T*** (L•g-1) is the binding constant, **R** (8.314 J•mol-1 •K-1) is the universal gas constant, **b_T** (J/mol) is the constant related to the heat of sorption, and **T** (°K) is temperature.

Whereas, Dubinin–Radushkevich's (D–R) isotherm model is expressed to calculate the Gaussian energy distribution. It can be applied on both homogenous and heterogeneous surfaces [72], which is expressed as:

$$\ln q_e = \ln q_{DR} - K_{DR} \varepsilon^2 \tag{12}$$

$$\varepsilon = RT \ln\left(1 + \frac{1}{Ce}\right) \tag{13}$$

$$E = \frac{1}{\sqrt{2B}} \tag{14}$$

where ***K_{DR}*** is a constant related to the mean free energy of adsorption, **q_{DR}** (mg/g) is the theoretical saturation capacity based on D–R isotherms and ***ε*** is the Polanyi potential. **T** is the absolute temperature (K) and **R** is the Boltzmann gas constant (8.314 J/mol K). **E** is the energy.

The data of regression value shown in Table 3 indicated that the best-fit isotherm models sequentially included Freundlich > Langmuir > Dubinin-Radushkevich > Temkin models.

The Freundlich isotherm model was the best fit model compared to other models for explaining the type of adsorbing metallic ions on the surface of the raw AV.

The Langmuir isotherm model Fig. 8 (a) was found as the second-best fit model in the fitting analysis. The Langmuir parameters were investigated based on equations (7) and (8). The RL value was found between 0 and 1 ($0 < R_L < 1$), which implies that the adsorption is favorable under the experimental conditions, and this result was in a good line with the Freundlich model about favorability results.

The Freundlich model Fig. 8 (b) is mainly based on the adsorption onto heterogeneous surfaces adsorption. It is known to have uneven accessible sites with different adsorption energies [31]. The parameter of the Freundlich model was analyzed based on equation (9). From the experiments, the value of 1/n followed **$0 < 1/n < 1$**, confirming that the adsorption occurred on the heterogeneous surface of the adsorbent

Table 2
Thermodynamic parameters of Cd(II) and Pb(II) adsorption onto AV at various temperatures.

Ion	ΔH° (KJ.mol^{-1})	ΔS° (J.mol^{-1}.K^{-1})	ΔG° (KJ.mol^{-1})			
			293 K	303 K	313 K	323 K
Cd (II)	1.912	15.555	−2.64	−2.79	−2.95	−2.98
Pb (II)	0.706	19.246	−4.932	−5.124	- 5.317	−5.509

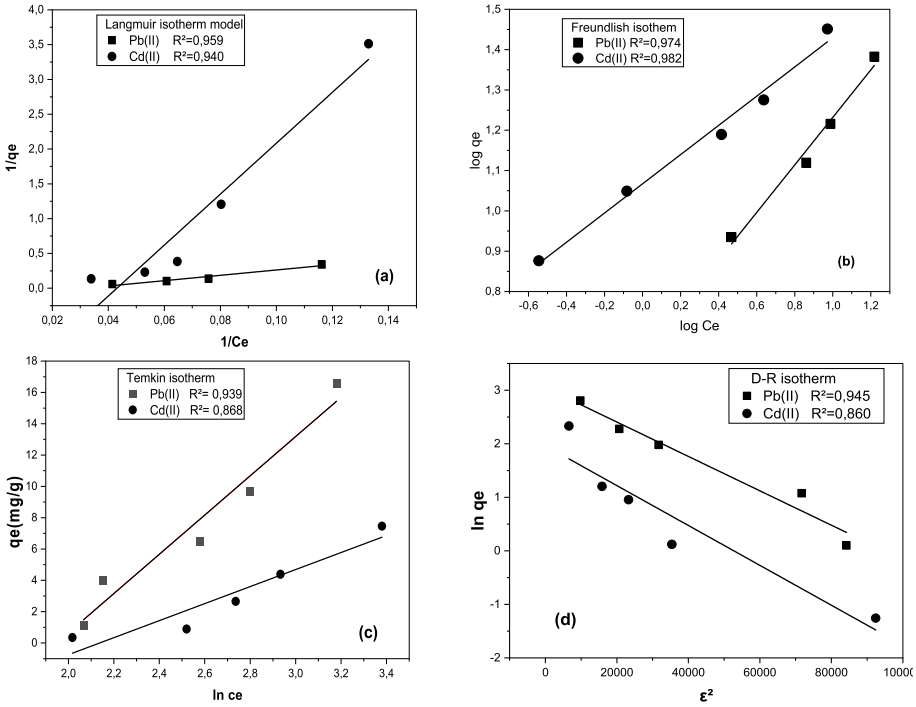

Fig. 8. Isotherm of adsorption of Pb(II) and Cd(II) **(a)** Langmuir, **(b)** Freundlich, **(c)**Temkin, **(d)** Dubinin–Radushkevich. ([M(II)] = 5.10^{-4} M; m_{ads} = 0.05 g; T = 20 °C).

Table 3
Isotherm adsorption models for Pb(II) and Cd(II) adsorption.

Isotherm Model	Parameters	Metallic ions	
		Pb(II)	Cd(II)
Langmuir	$\mathbf{q_m}$ (mg•g^{-1})	17.54	2.28
	$\mathbf{K_L}$ (L•mg^{-1})	0.031	0.042
	$\mathbf{R_L}$	0.145	0.186
	$\mathbf{R^2}$	**0.94**	**0.92**
Freundlich	**1/n**	0.58	0.36
	$\mathbf{K_f}$ **(mg$^{1-1/n}$L$^{1/n}$g^{-1})**	4.36	11.66
	$\mathbf{R^2}$	**0.97**	**0.98**
Temkin	**B**	12.53	5.43
	$\mathbf{A_T}$ (L•g^{-1})	0.141	0.115
	$\mathbf{b_T}$ (J•mol^{-1})	194.41	448.61
	$\mathbf{R^2}$	**0.93**	**0.86**
Dubinin- Radushkevich (D-R)	$K_{D\text{-}R}$ (mol^2/Kj^2)	3.21	3.72
	$q_{m\ D\text{-}R}$ (mg/g)	21.05	7.09
	E (Kj/mol)	0.394	0.366
	$\mathbf{R^2}$	**0.94**	**0.86**

(Table 3). The values of the coefficient **1/n** are less than 1, which is characteristic of normal adsorption. The **n** value obtained in this study was higher than 1, which shows favorable physical adsorption [73,74].

The parameter of the Temkin model Fig. 8(c) was studied using equations (10) and (11). Temkin is characterized by the uniform distribution of binding energies. $\mathbf{b_T}$ value indicated that b_T < 8 kJ/mol, indicating physical adsorption (physisorption). The R2 value is high, which means that this isotherm is adequate for this study.

Linear fitting from the Dubinin-Radushkevich model was analyzed for obtaining the parameters' values based on equations (12), **(13)**, and **(14)**. The linear fitting analysis showed E < 8 kJ/mol, confirming that the type of adsorption of Pb (II) and Cd(II) onto the biosorbent followed a physical process.

Based on these isotherms model parameters, the adsorption of metallic cations onto the raw AV surface was a physical process. The adsorbate molecules were attracted to the adsorption site through the van der Waals force [75,76].

3.5. *Kinetics models*

The adsorption kinetics of Pb(II) and Cd(II) by the raw aloe vera were explained and evaluated by using pseudo-first-order (PFO) (Eq. (15)), pseudo-second-order (PSO)(Eq. (16)), and intraparticle diffusion (the Weber–Morris) (Eq. (17)) and Elovich (Eq. (18)) models [73,77].

The linear formula of these models can be written using the following equations:

$$\mathbf{Ln(q_e - q_t) = -k_1.t + Ln\ q_e} \tag{15}$$

$$\frac{\mathbf{t}}{\mathbf{qt}} = \frac{1}{\mathbf{K_2.qe^2}} + \frac{\mathbf{t}}{\mathbf{qe}} \tag{16}$$

$$\mathbf{q_t = k_{int} t^{1/2} + C} \tag{17}$$

$$\mathbf{q_t = \frac{1}{\beta}\ln(\alpha\beta) + \frac{1}{\beta}\ln(t)} \tag{18}$$

where $\mathbf{k_1}$ and $\mathbf{k_2}$(g.mg^{-1}.min^{-1}) are the equilibrium rate constants of

(PFO) (min^{-1}) and (PSO) models respectively. **qe** and **qt** ($mg \cdot g^{-1}$) are the adsorption capacity at equilibrium and at time t, respectively, **C** is the maximum adsorption amount, and $\mathbf{k_{int}}$ is the intraparticle diffusion rate constant ($g \cdot mg^{-1}\ min^{-1}$).

The Elovich model is used to predict the sorption mechanism, where **qt** is adsorbed quantity at time **t**, while **α** and **β** are initial sorption concentration rate ($mg \cdot g^{-1}.min^{-1}$) and desorption constant (g/mg), respectively.

These models are represented in Fig. 9, and the correlation coefficients and parameter values calculated from the four kinetic models are summarized in Table 4.

The experimental results showed that the pseudo-second order (PSO) model is the best fitted to the experimental data than other kinetic models. The correlation coefficient values (R^2) of PSO kinetic model are the highest for both cations, and are closer to unity compared to other models. Furthermore, the experimental values of the adsorption capacity (qe_{exp}) at equilibrium 16.55 and 8.25 mg/g were found to be in excellent agreement with the calculated values from the second-order kinetic equation (PSO) 17.54 and 7.35 mg/g for Pb(II) and Cd(II), respectively. These values confirm the validity of the (PSO) to evaluate the adsorption of these metallic cations from the aqueous solution by the AV adsorbent. From the pseudo-first-order model (PFO) predicted a significantly lower value of the calculated equilibrium adsorption capacity (qe, cal) than the experimental value (qe, exp), indicating the inapplicability of this model.

Based on these results, it can be concluded that the (PSO) adsorption mechanism is predominant and more suitable to describe the adsorption kinetics of these metal ions by the raw aloe vera material. The experimental data were in good agreement with the PSO model [62–67,78,79].

On the other hand, in the Weber-Morris model, the values of $C \neq 0$, and the coefficient of determination ($R^2 = 0.742$ and 0.855) is not satisfactory, indicating that the intra-particle diffusion is not the rate-limiting step in the determination of the kinetic process.

According to the Elovich model shown in Fig. 9(d), the high R2 values (0.95 and 0.91) for Pb(II) and Cd(II)were relatively high indicating that Elovich model is suitable for modeling the adsorption process and show that the desorption rate was higher than the initial sorption [54,67].

Table 4
Calculated parameters of the kinetic models for Pb(II) and Cd(II) adsorption.

Kenetic models	Parameters	Pb(II)	Cd(II)
	qe .Exp ($mg.g^{-1}$)	16.55	8.25
pseudo first order	**qe,cal ($mg.g^{-1}$)**	0.761	0.260
	k_1 (min^{-1})	0.185	0.0672
	R^2	**0.766**	**0.879**
pseudo second order	**k_2 ($g.mg^{-1}.min^{-1}$)**	0.147	0.0587
	qe,cal ($mg.g^{-1}$)	17.54	7.35
	R^2	**0.999**	**0.997**
Weber-Morris (Intraparticle diffusion)	**K_i ($g.mg^{-1}.min^{-1}$)**	0.157	0.422
	C ($mg.g^{-1}$)	15.88	6.406
	R^2	**0.742**	**0.855**
Elovich model	**β** (g. mg^{-1})		
	α (mg. g^{-1} min^{-1})		
	R^2		

3.6. Computational methods

3.6.1. DFT and Frontier molecular orbital results

All the structures were built using the GaussView software package; the chemical structures of these molecules are displayed in Fig. 10. DFT calculations were performed with the Orca program with the B97-D3 and 6-311++G**//LANL2DZ basis sets to optimize the complex using the implicit solvation models SMD (Solvation Model based on density).

Frontier molecular orbital analysis (FMO) is imperative parameters used to largely explain how the monomeric atoms of Pb and Cd interact with the compound AV in the complex (AV@(Pb//Cd)), and to give more information about the quality of the chemical stability of the complexes, as well as the region from which the adsorption has strong non-covalent electrostatic interactions, as shown in Fig. 11. it can be said that the FMO analysis serves to characterize in the region of the

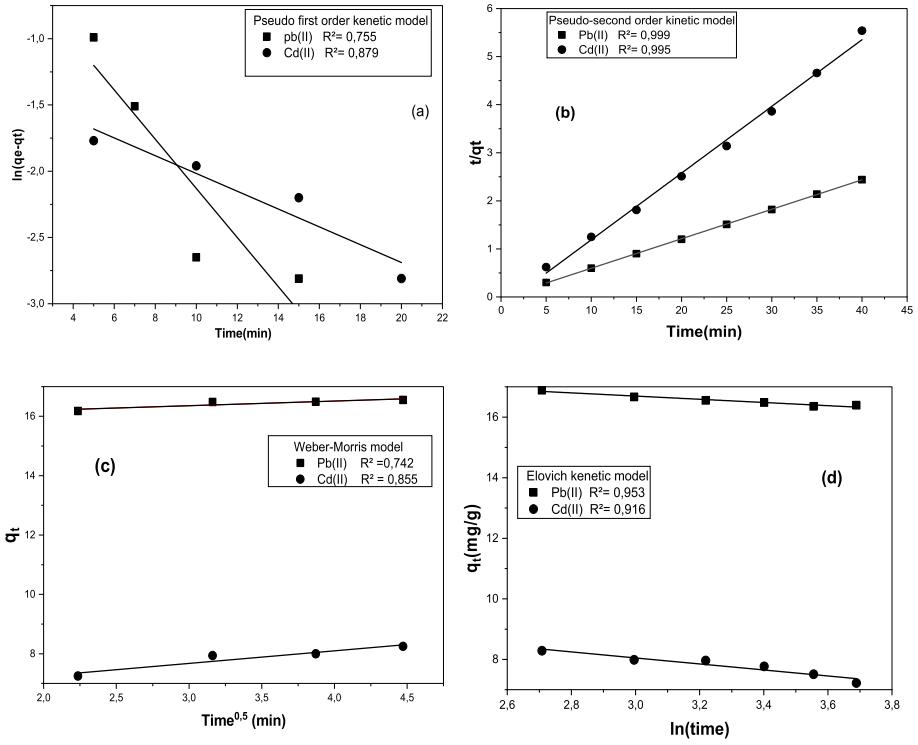

Fig. 9. Kinetic model for Pb (II) and Cd(II) adsorption. **(a)** Pseudo-frst-order,**(b)** pseudo-second order and **(c)** Weber-Morris model (intraparticle diffusion); ([M(II)] = 5.10^{-4} M; contact time = 5–40 min T = 20 °C).

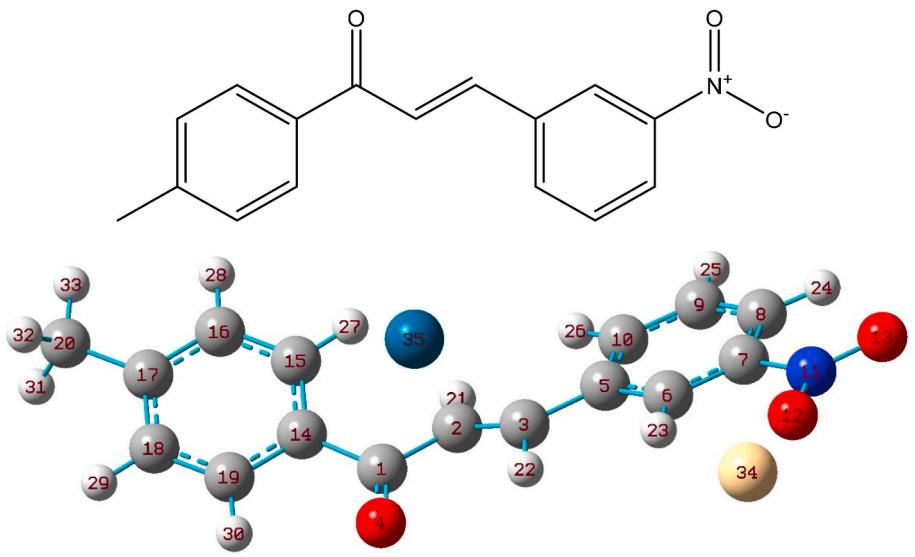

Fig. 10. The chemical structures (2D and 3D) of the complex optimized using DFT//B97D3/6-311++G**/land2dz level of theory, (color symbol; O: red, N: blue, Cd: yellow, C: cyan,Pb: green and H: white). (For interpretation of the references to color in this figure legend, the reader is referred to the Web version of this article.)

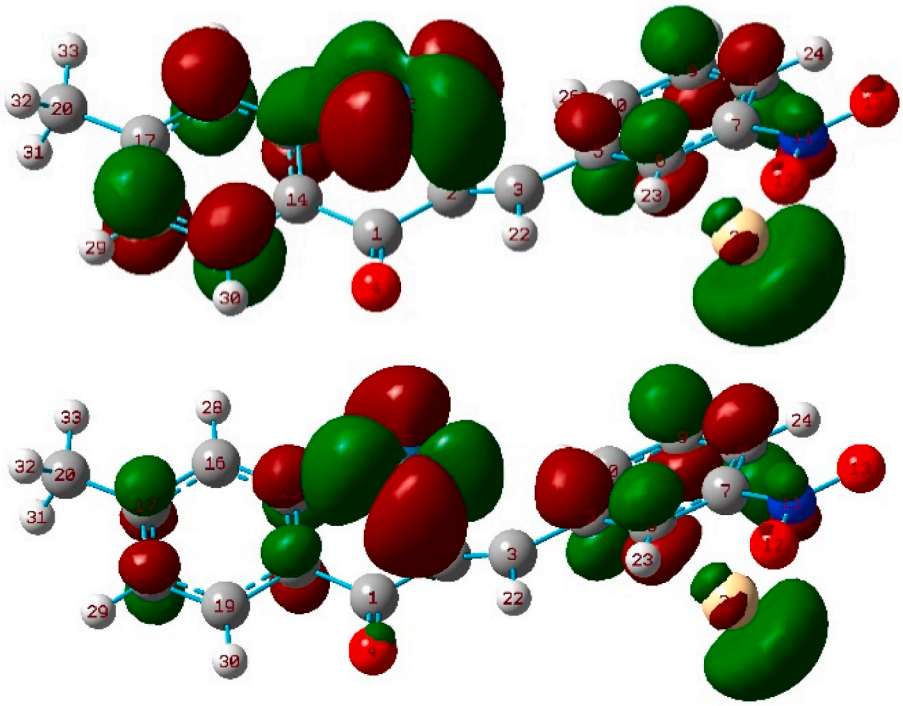

Fig. 11. DFTcalculated for HOMO (left) and LUMO (right) frontier orbitals for complex of (AV@(Pb//Cd))

charge distribution around the bond formed that is asymmetrically centered visualized by large red and green spots, which made a significant contribution to the electronic transition used to stabilize the complex Table 5.

In other part, based on natural bond orbital (NBO) analysis, the delocalization of charge from donors (Aloe Vera) to acceptor level (heavy atoms Pb and Cd) has been investigated by examining all possible interactions from donors to acceptor orbitals or known bonding and antibonding interaction. The stability of the molecular system is determined by stabilization energy E(2) which is associated with the i to j delocalization involving the lone pair donor i and acceptor j orbitals. Form NBO results, the negative charge on carbon atom C_2(−0.16980) and C_6(−0.19975) are strongly delocalized with the carbonyl groups (C=O_4(−0.22636)) and via charge transfer interactions with Pb (0.3035) and Cd (0.46986), that involving their energetic importance by 2nd-order perturbation theory.E(2) = 46.33 kcal/mol for nC_2-Pb→π^*C_1–O_4 and 43.67 kcal/mol π^*C_6–Cd→LP*Cd, which confirmed the stability of the complex.

4. Conclusion

The results revealed that the potential of the raw Aloe Vera leaves has the advantage of being available, cheap, and economical and has the power to remove hazardous metals like cadmium and lead from an aqueous solution by an effortless and efficient method as the adsorption procedure that might be of interest for industrial and for environmental

Table 5
Natural Population Analysis and Fukui indices calculated of all (AV@Pb// Cdcomplex) atoms by B97D3/6-311++G**/land2dz in the presence of the water solvent by theimplicit solvation model SMD.

Atome k	qk(M)	qk(M+)	qk(M −)	f+	f-
Cd 34	0.46986	0.76003	0.47251	0.29017	−0.00265
Pb 35	0.30350	0.46494	−0.02292	0.16144	0.32642
O 13	−0.17151	−0.05750	−0.2302	0.11401	0.05869
O 12	−0.18753	−0.12084	−0.28226	0.06669	0.09473
N 11	0.06833	0.12151	0.04533	0.05318	0.02300
C 9	−0.06875	−0.0250	−0.06094	0.04375	−0.00781
H 25	0.05861	0.09197	0.03355	0.03336	0.02506
C 7	−0.08148	−0.05071	−0.0536	0.03077	−0.02788
C 5	0.02623	0.05699	0.04206	0.03076	−0.01583
H 26	0.05364	0.08018	0.03470	0.02654	0.01894
H 24	0.07691	0.10150	0.05137	0.02459	0.02554
O 4	−0.22636	−0.20198	−0.27065	0.02438	0.04429
C 10	−0.05158	−0.03314	−0.10767	0.01844	0.05609
C 17	0.04023	0.05831	0.0119	0.01808	0.02833
C 2	−0.16980	−0.15638	−0.21076	0.01342	0.04096
H 29	0.05264	0.06606	0.03276	0.01342	0.01988
H 21	0.05581	0.06614	0.03598	0.01033	0.01983
H 28	0.05104	0.06131	0.0348	0.01027	0.01624
H 31	0.06905	0.07890	0.05441	0.00985	0.01464
C 18	−0.06024	−0.05082	−0.07183	0.00942	0.01159
H 32	0.06875	0.07730	0.05676	0.00855	0.01199
C 19	−0.05195	−0.04405	−0.07119	0.00790	0.01924
H 30	0.06308	0.07038	0.04940	0.00730	0.01368
C 8	−0.06261	−0.05548	−0.11721	0.00713	0.0546
C 1	0.10035	0.10723	0.07850	0.00688	0.02185
H 33	0.06343	0.06992	0.05378	0.00649	0.00965
H 23	0.09472	0.10099	0.07632	0.00627	0.0184
H 22	0.05902	0.06525	0.04089	0.00623	0.01813
C 16	−0.06321	−0.05799	−0.07574	0.00522	0.01253
C 15	−0.06802	−0.07003	−0.06058	−0.00201	−0.00744
H 27	0.05012	0.04713	0.05090	−0.00299	−0.00078
C 20	−0.18881	−0.19254	−0.1832	−0.00373	−0.00561
C 14	−0.03356	−0.04345	−0.01768	−0.00989	−0.01588
C 3	−0.14018	−0.15774	−0.16827	−0.01756	0.02809
C 6	−0.19975	−0.22839	−0.25124	−0.02864	0.05149

applications for the removal of toxic metal ions from the environment.

The present study has shown that the mechanism of adsorption of these metals by AV is dependent on the pH of the solution, at acidic pH, the Pb ions adsorption is favored with an adsorption yield of 95.79%, while Cd ions offer a good retention capacity at initial pH 6 reached 81.54%.

Moreover, the increase in metallic concentration and the AV mass decreases the adsorption process.Thermodynamic studies have proven that the removal of Pb (II) and Cd (II) is spontaneous, and endothermic with the mechanism of physical adsorption.

Kinetic models indicate that the PSO model better describes the adsorption kinetics of these ions and the isotherm adsorption was most accurately described by the Freundlich model.

DFT calculations were carried out by using the functional B97D3 and 6-311++G** land2dz basis set with the SMD implicit solvent model.

The geometry optimization, the local reactivity descriptor, and the NBO analysis has been concluded that the atoms C_2, C_3, $C_6$and N_{11} are close to nucleophilic center.

Acknowledgments

The financial support for this work from the General Directorate of Scientific Research and Technological Development (DGRSDT) and the Ministry of Higher Education and Scientific Research is appreciated. The authors also thank the European Institute of Membranes Université Montpellier, France, for carrying out this work.

This work was supported by Dr Moulay Tahar University, Saïda, Algeria and the “PunchOrga” Network (Normand University Pole of Organic Chemistry), the “Ministry of Research and New Technologies”, CNRS (National Research Center Scientist).

References

[1] M.A. Habila, Z.A. ALOthman, A.M. El-Toni, J.P. Labis, M. Soylak, Synthesis and application of Fe3O4@ SiO2@ TiO2 for photocatalytic decomposition of organic matrix simultaneously with magnetic solid phase extraction of heavy metals prior to ICP-MS analysis, Talanta 154 (2016) 539–547, https://doi.org/10.1016/j.talanta.2016.03.081.

[2] M.M. Musameh, M. Hickey, I.L. Kyratzis, Carbon nanotube-based extraction and electrochemical detection of heavy metals, Res. Chem. Intermed. 37 (7) (2011) 675–689, https://doi.org/10.1007/s11164-011-0307-x.

[3] K. Singh, S.K. Sharma, A. Jain, M. Mandal, P.K. Pandey, Removal of copper ion from synthetic wastewater using Aloe vera as an adsorbent, Eur. J. Adv. Eng. Technol. 4 (4) (2017) 249–254.

[4] P.O. Patil, P.V. Bhandari, P.K. Deshmukh, S.S. Mahale, A.G. Patil, H.R. Bafna, K. V. Patel, S.B. Bari, Green fabrication of graphene-based silver nanocomposites using agro-waste for sensing of heavy metals, Res. Chem. Intermed. 43 (7) (2017) 3757–3773, https://doi.org/10.1007/s11164-016-2844-9.

[5] R. Upstill-Goddard, P.J. WANGERSKY (Eds.), Marine Chemistry. Pollution. The Handbook of Environmental Chemistry, 5D, Cambridge University Press Cambridge Core, 2000 xiv+230 pp. Berlin, Heidelberg, New York, London, Paris, Tokyo, Hong Kong: Springer-Verlag. Price DM 189.00, SFr 163.00, £65.00, US $109.99 (hard covers). ISBN 3 540 66020 8. Geological Magazine 2002, 139 (3), 365-372. DOI: 10.1017/S0016756802276694 From.

[6] W. Janusz, V. Sydorchuk, E. Skwarek, S. Khalameida, Effect of hydrothermal treatment of zirconium phosphate xerogel on its surface groups properties and affinity adsorption to Cd (II) ions from acidic solutions, Mater. Res. Bull. 148 (2022), 111674, https://doi.org/10.1016/j.materresbull.2021.111674.

[7] V.K. Gupta, M.L. Yola, N. Atar, Z. Ustundağ, A.O. Solak, A novel sensitive Cu(II) and Cd(II) nanosensor platform: graphene oxide terminated p-aminophenyl modified glassy carbon surface, Electrochim. Acta 112 (2013) 541–548, https://doi.org/10.1016/j.electacta.2013.09.011.

[8] R.D. Ambashta, M. Sillanpää, Water purification using magnetic assistance: a review, J. Hazard Mater. 180 (1) (2010) 38–49, https://doi.org/10.1016/j.jhazmat.2010.04.105.

[9] Y.-H. Li, Z. Di, J. Ding, D. Wu, Z. Luan, Y. Zhu, Adsorption thermodynamic, kinetic and desorption studies of Pb2+ on carbon nanotubes, Water Res. 39 (4) (2005) 605–609, https://doi.org/10.1016/j.watres.2004.11.004.

[10] I. Djamila, M. Kaid, Z. Hanane, D. Villemein, Spectrophotometric study of Solvent extraction of Pb (II) and Cd (II) by aminooctyldiphosphonic acid [version 1; peer review: awaiting peer review], F1000Research 10 (1140) (2021), https://doi.org/10.12688/f1000research.54030.1.

[11] C. Luo, R. Wei, D. Guo, S. Zhang, S. Yan, Adsorption behavior of MnO2 functionalized multi-walled carbon nanotubes for the removal of cadmium from aqueous solutions, Chem. Eng. J. 225 (2013) 406–415, https://doi.org/10.1016/j.cej.2013.03.128.

[12] R. Malik, S. Lata, S. Singhal, Removal of heavy metal from wastewater by the use of modified aloe vera leaf powder, Int. J. Basic Appl. Chem. Sci. 5 (2) (2015) 6–17.

[13] F. Fu, Q. Wang, Removal of heavy metal ions from wastewaters: a review, J. Environ. Manag. 92 (3) (2011) 407–418, https://doi.org/10.1016/j.jenvman.2010.11.011.

[14] A. Kadeche, A. Ramdani, M. Adjdir, A. Guendouzi, S. Taleb, M. Kaid, A. Deratani, Preparation, characterization and application of Fe-pillared bentonite to the removal of Coomassie blue dye from aqueous solutions, Res. Chem. Intermed. 46 (11) (2020) 4985–5008, https://doi.org/10.1007/s11164-020-04236-2.

[15] T. Bohli, A. Ouederni, N. Fiol, I. Villaescusa, Single and binary adsorption of some heavy metal ions from aqueous solutions by activated carbon derived from olive stones, Desalination Water Treat. 53 (4) (2015) 1082–1088, https://doi.org/10.1080/19443994.2013.859099.

[16] M.A. Hashem, Adsorption of lead ions from aqueous solution by okra wastes, Int. J. Phys. Sci. 2 (7) (2007) 178–184, https://doi.org/10.5897/IJPS.9000050.

[17] M. Ahmaruzzaman, Industrial wastes as low-cost potential adsorbents for the treatment of wastewater laden with heavy metals, Adv. Colloid Interface Sci. 166 (1) (2011) 36–59, https://doi.org/10.1016/j.cis.2011.04.005.

[18] T.A. Kurniawan, G.Y.S. Chan, W.-h. Lo, S. Babel, Comparisons of low-cost adsorbents for treating wastewaters laden with heavy metals, Sci. Total Environ. 366 (2) (2006) 409–426, https://doi.org/10.1016/j.scitotenv.2005.10.001.

[19] D. Sud, G. Mahajan, M.P. Kaur, Agricultural waste material as potential adsorbent for sequestering heavy metal ions from aqueous solutions – a review, Bioresour. Technol. 99 (14) (2008) 6017–6027, https://doi.org/10.1016/j.biortech.2007.11.064.

[20] T.M. Zewail, S.A.M. El-Garf, Preparation of agriculture residue based adsorbents for heavy metal removal, Desalination Water Treat. 22 (1–3) (2010) 363–370, https://doi.org/10.5004/dwt.2010.1245.

[21] A. Biedrzycka, E. Skwarek, U.M. Hanna, Hydroxyapatite with magnetic core: synthesis methods, properties, adsorption and medical applications, Adv. Colloid Interface Sci. 291 (2021), 102401, https://doi.org/10.1016/j.cis.2021.102401.

[22] S. Abedi, H. Zavvar Mousavi, A. Asghari, Investigation of heavy metal ions adsorption by magnetically modified aloe vera leaves ash based on equilibrium, kinetic and thermodynamic studies, Desalination Water Treat. 57 (29) (2016) 13747–13759, https://doi.org/10.1080/19443994.2015.1060536.

[23] H. Singh, G. Chauhan, A.K. Jain, S.K. Sharma, Adsorptive potential of agricultural wastes for removal of dyes from aqueous solutions, J. Environ. Chem. Eng. 5 (1) (2017) 122–135, https://doi.org/10.1016/j.jece.2016.11.030.

[24] I. Slatni, F.Z. Elberrichi, J. Duplay, N.E.H. Fardjaoui, A. Guendouzi, O. Guendouzi, B. Gasmi, F. Akbal, I. Rekkab, Mesoporous silica synthesized from natural local kaolin as an effective adsorbent for removing of Acid Red 337 and its application in

the treatment of real industrial textile effluent, Environ. Sci. Pollut. Control Ser. 27 (31) (2020) 38422–38433, https://doi.org/10.1007/s11356-020-08615-5.
[25] A.A. Moosa, A.M. Ridha, N.A. Hussien, Removal of zinc ions from aqueous solution by bioadsorbents and CNTs, Am. J. Mater. Sci. 6 (4) (2016) 105–114, https://doi.org/10.5923/j.materials.20160604.04.
[26] V. Tripathi, S. Srivastava, A. Dwivedi, Aloe vera Burm. F. A potential botanical tool for bioremediation of arsenic, Sch. J. Agric. Vet. Sci. 3 (7) (2016), https://doi.org/10.21276/sjavs.2016.3.7.6.
[27] C. Pragathiswaran, S. Sibi, P. Sivanesan, Removal of Cr (VI) from aqueous solution using Eihhornea Crassipies: characteristic and equilibrium study, Int. J. Res. Pharm. Chem. 3 (4) (2013) 863–865. http://ijrpc.com/files/23-3221.pdf.
[28] S. Murakami, K. Ogura, T. Yoshino, Equilibria of complex formation between Bivalent metal ions and 3,3′-bis[N,N′-bis(carboxymethyl)aminomethyl]-o-cresolsulfonphthalein, Bull. Chem. Soc. Jpn. 53 (8) (1980) 2228–2235, https://doi.org/10.1246/bcsj.53.2228, acccessed 2022/05/07.
[29] C. Lee, W. Yang, R.G. Parr, Development of the Colle-Salvetti correlation-energy formula into a functional of the electron density, Phys. Rev. B 37 (2) (1988) 785–789, https://doi.org/10.1103/PhysRevB.37.785.
[30] P. Hohenberg, W. Kohn, Inhomogeneous electron gas, Phys. Rev. 136 (3B) (1964) B864–B871, https://doi.org/10.1103/PhysRev.136.B864.
[31] A. Ramdani, Z. Taleb, A. Guendouzi, A. Kadeche, H. Herbache, A. Mostefai, S. Taleb, A. Deratani, Mechanism study of metal ion adsorption on porous hydroxyapatite: experiments and modeling, Can. J. Chem. 98 (2) (2020) 79–89, https://doi.org/10.1139/cjc-2019-0315.
[32] C. Xu, S. Zhou, J. Chen, Y. Wang, L. He, Adsorption mechanism of CO molecule on Al(111) surface: periodic DFT investigation, Can. J. Chem. 96 (12) (2018) 993–999, https://doi.org/10.1139/cjc-2018-0169.
[33] R. Dennington, T. Keith, J.G. Millam, Version 5, Semichem Inc, Shawnee Mission, KS, USA, 2009. GaussView, Version 5.
[34] Neese, F. Software update: the ORCA program system, version 4.0. WIREs Computat. Mol. Sci. 2018, 8 (1), e1327, https://doi.org/10.1002/wcms.1327. DOI: https://doi.org/10.1002/wcms.1327 (acccessed 2022/05/07).
[35] J.S. Binkley, J.A. Pople, W.J. Hehre, Self-consistent molecular orbital methods. 21. Small split-valence basis sets for first-row elements, J. Am. Chem. Soc. 102 (3) (1980) 939–947, https://doi.org/10.1021/ja00523a008.
[36] Grimme, S.; Ehrlich, S.; Goerigk, L. Effect of the damping function in dispersion corrected density functional theory. J. Comput. Chem. 2011, 32 (7), 1456-1465, https://doi.org/10.1002/jcc.21759. DOI: https://doi.org/10.1002/jcc.21759 (acccessed 2022/05/07).
[37] A.V. Marenich, C.J. Cramer, D.G. Truhlar, Universal solvation model based on solute electron density and on a continuum model of the solvent defined by the Bulk dielectric constant and atomic surface tensions, J. Phys. Chem. B 113 (18) (2009) 6378–6396, https://doi.org/10.1021/jp810292n.
[38] S. Grimme, J. Antony, S. Ehrlich, H. Krieg, A consistent and accurate ab initio parametrization of density functional dispersion correction (DFT-D) for the 94 elements H-Pu, J. Chem. Phys. 132 (15) (2010) 154104, https://doi.org/10.1063/1.3382344.
[39] P. Jithendra, A.M. Rajam, T. Kalaivani, A.B. Mandal, C. Rose, Preparation and characterization of aloe vera Blended Collagen-Chitosan composite scaffold for tissue engineering applications, ACS Appl. Mater. Interfaces 5 (15) (2013) 7291–7298, https://doi.org/10.1021/am401637c.
[40] Z.X. Lim, K.Y. Cheong, Effects of drying temperature and ethanol concentration on bipolar switching characteristics of natural Aloe vera-based memory devices, Phys. Chem. Chem. Phys. 17 (40) (2015) 26833–26853, https://doi.org/10.1039/C5CP04622J.
[41] F. Nejatzadeh-Barandozi, S.T. Enferadi, FT-IR study of the polysaccharides isolated from the skin juice, gel juice, and flower of Aloe vera tissues affected by fertilizer treatment, Org. Med. Chem. Lett. 2 (1) (2012) 33, https://doi.org/10.1186/2191-2858-2-33.
[42] N. Ertugay, Y.K. Bayhan, Biosorption of Cr (VI) from aqueous solutions by biomass of Agaricus bisporus, J. Hazard Mater. 154 (1) (2008) 432–439, https://doi.org/10.1016/j.jhazmat.2007.10.070.
[43] S. Pradhan, S. Singh, L.C. Rai, Characterization of various functional groups present in the capsule of Microcystis and study of their role in biosorption of Fe, Ni and Cr, Bioresour. Technol. 98 (3) (2007) 595–601, https://doi.org/10.1016/j.biortech.2006.02.041.
[44] V. Veeraganesh, A. Subramaniyan, T. Sornakumar, Effect of Aloe vera on synthesis of nano Tin (iv) oxide, Asian J. Nanosci. Mater. 1 (3) (2018) 115–121.
[45] O.D. Uluozlu, A. Sarı, M. Tuzen, Biosorption of antimony from aqueous solution by lichen (Physcia tribacia) biomass, Chem. Eng. J. 163 (3) (2010) 382–388, https://doi.org/10.1016/j.cej.2010.08.022.
[46] S. Cheng, S. Panthapulakkal, M. Sain, A. Asiri, Aloe vera rind cellulose nanofibers-reinforced films, J. Appl. Polym. Sci. 131 (15) (2014), https://doi.org/10.1002/app.40592.
[47] A. Mostafaei, A. Zolriasatein, Synthesis and characterization of conducting polyaniline nanocomposites containing ZnO nanorods, Prog. Nat. Sci.: Mater. Int. 22 (4) (2012) 273–280, https://doi.org/10.1016/j.pnsc.2012.07.002.
[48] L.I. Nadaf, K.S. Venkatesh, Polyaniline-copper oxide nano-composites: synthesis and characterization, Mater. Sci. Res. India 12 (2) (2015) 108–111, https://doi.org/10.13005/msri/120204.
[49] L. Yesappa, M. Niranjana, S.P. Ashokkumar, H. Vijeth, C. Sharanappa, S. Raghu, H. Devendrappa, Synthesis, characterization and absorption study of aloe vera doped polyaniline Bio-composite, Mater. Today Proc. 5 (10, Part 1) (2018) 21076–21081, https://doi.org/10.1016/j.matpr.2018.06.502.
[50] I.E. Uwah, A.I. Ikeuba, B.U. Ugi, V.M. Udowo, Comparative study of the inhibition effects of alkaloid and non alkaloid fractions of the ethanolic extracts of Costus afer stem on the corrosion of mild steel in 5 M HCl solution, Global J. Pure Appl. Sci. 19 (1) (2013) 23–31, https://doi.org/10.4314/gjpas.v19i1.4.
[51] D.L. Kouadio, M. Diarra, B.T.D. Tra, D.P.V. Akesse, B.D. Soro, K.N. Aboua, L. Meite, M. Kone, A. Dembele, K.S. Traore, Adsorption du colorant textile Jaune 11 sur du charbon actif issue de la coque d'arachide, Int. J. Innovat. Appl. Stud. 26 (4) (2019) 1280–1292.
[52] S. Gupta, A. Kumar, Removal of nickel (II) from aqueous solution by biosorption on A. barbadensis Miller waste leaves powder, Appl. Water Sci. 9 (4) (2019) 96, https://doi.org/10.1007/s13201-019-0973-1.
[53] D.I. Fox, Cactus Mucilage-Assisted Heavy Metal Separation: Design and Implementation, University of South Florida, 2011.
[54] D. Ozdes, C. Duran, H.B. Senturk, Adsorptive removal of Cd(II) and Pb(II) ions from aqueous solutions by using Turkish illitic clay, J. Environ. Manag. 92 (12) (2011) 3082–3090, https://doi.org/10.1016/j.jenvman.2011.07.022.
[55] I. Puigdomenech, HYDRA (Hydrochemical Equilibrium-Constant Database) and MEDUSA (Make Equilibrium Diagrams Using Sophisticated Algorithms) Programs, Royal Institute of Technology, Sweden, 2006. http://www.kemi.kth.se/medusa.
[56] N.C. Joshi, N. Malik, A. Singh, Synthesis and characterizations of polythiophene–Al2O3 based nanosorbent and its applications in the removal of Pb2+, Cd2+ and Zn2+ ions, J. Inorg. Organomet. Polym. Mater. 30 (4) (2020) 1438–1447, https://doi.org/10.1007/s10904-019-01252-7.
[57] A. Parus, K. Wieszczycka, A. Olszanowski, Solvent extraction of cadmium(II) from chloride solutions by pyridyl ketoximes, Hydrometallurgy 105 (3) (2011) 284–289, https://doi.org/10.1016/j.hydromet.2010.10.007.
[58] M. Pourbaix, H. Zhang, X. Yang, Atlas of chemical and electrochemical equilibria in the presence of a gaseous phase, Cebelcor (1996).
[59] A.A. Baba, F.A. Adekola, Solvent extraction of Pb(II) and Zn(II) from a Nigerian galena ore leach liquor by tributylphosphate and bis(2,4,4-trimethylpentyl) phosphinic acid, J. King Saud Univ. Sci. 25 (4) (2013) 297–305, https://doi.org/10.1016/j.jksus.2013.07.003.
[60] A. SÖNmezay, M.S. ÖNcel, N. BektaŞ, Adsorption of lead and cadmium ions from aqueous solutions using manganoxide minerals, Trans. Nonferrous Metals Soc. China 22 (12) (2012) 3131–3139, https://doi.org/10.1016/S1003-6326(12)61765-8.
[61] M. Kadari, M.h. Kaid, M. Ben Ali, D. Villemin, Selective study of elimination of Cd (II) and Pb (II) from aqueous solution by novel hybrid material, J. Chin. Adv. Mater. Soc. 5 (3) (2017) 149–157, https://doi.org/10.1080/22243682.2017.1329027.
[62] A. Babarinde, K. Ogundipe, K.T. Sangosanya, B.D. Akintola, A.O.E. Hassan, Comparative study on the biosorption of Pb (II), Cd (II) and Zn (II) using Lemon grass (Cymbopogon citratus): kinetics, isotherms and thermodynamics, Chem. Int. 2 (8) (2016) 89–102.
[63] M. El-Azazy, S.N. Dimassi, A.S. El-Shafie, A.A. Issa, Bio-Waste aloe vera leaves as an efficient adsorbent for Titan yellow from wastewater: structuring of a novel adsorbent using plackett-Burman factorial design, Appl. Sci. 9 (22) (2019) 4856.
[64] E.A. Ofudje, I.A. Adeogun, M.A. Idowu, S.O. Kareem, N.A. Ndukwe, Simultaneous removals of cadmium(II) ions and reactive yellow 4 dye from aqueous solution by bone meal-derived apatite: kinetics, equilibrium and thermodynamic evaluations, J. Anal. Sci. Technol. 11 (1) (2020) 7, https://doi.org/10.1186/s40543-020-0206-0.
[65] L. He, D.-D. Liu, B.-B. Wang, H.-B. Xu, Removal of heavy metals from aqueous solution by poly(ethyleneimine)-functionalized silica: studies on equilibrium isotherm, kinetics, and thermodynamics of interactions, Res. Chem. Intermed. 41 (6) (2015) 3913–3928, https://doi.org/10.1007/s11164-013-1499-z.
[66] Z. Wang, G. Huang, C. An, L. Chen, J. Liu, Removal of copper, zinc and cadmium ions through adsorption on water-quenched blast furnace slag, Desalination Water Treat. 57 (47) (2016) 22493–22506, https://doi.org/10.1080/19443994.2015.1135084.
[67] W. Boulaiche, B. Hamdi, M. Trari, Removal of heavy metals by chitin: equilibrium, kinetic and thermodynamic studies, Appl. Water Sci. 9 (2) (2019) 39, https://doi.org/10.1007/s13201-019-0926-8.
[68] R.M. Ali, H.A. Hamad, M.M. Hussein, G.F. Malash, Potential of using green adsorbent of heavy metal removal from aqueous solutions: adsorption kinetics, isotherm, thermodynamic, mechanism and economic analysis, Ecol. Eng. 91 (2016) 317–332, https://doi.org/10.1016/j.ecoleng.2016.03.015.
[69] H.-K. Chung, W.-H. Kim, J. Park, J. Cho, T.-Y. Jeong, P.-K. Park, Application of Langmuir and Freundlich isotherms to predict adsorbate removal efficiency or required amount of adsorbent, J. Ind. Eng. Chem. 28 (2015) 241–246, https://doi.org/10.1016/j.jiec.2015.02.021.
[70] A.B.D. Nandiyanto, S.-G. Kim, F. Iskandar, K. Okuyama, Synthesis of spherical mesoporous silica nanoparticles with nanometer-size controllable pores and outer diameters, Microporous Mesoporous Mater. 120 (3) (2009) 447–453, https://doi.org/10.1016/j.micromeso.2008.12.019.
[71] N. Ayawei, A.N. Ebelegi, D. Wankasi, Modelling and interpretation of adsorption isotherms, J. Chem. 2017 (2017) 3039817, https://doi.org/10.1155/2017/3039817.
[72] A.B.D. Nandiyanto, R. Andika, M. Aziz, L.S. Riza, Working volume and milling time on the product size/morphology, product yield, and electricity consumption in the ball-milling process of organic material, Indones. J. Sci. Technol. 3 (2018) 82–94.
[73] G. Sharma, M. Naushad, A. Kumar, S. Rana, S. Sharma, A. Bhatnagar, F.J. Stadler, A.A. Ghfar, M.R. Khan, Efficient removal of coomassie brilliant blue R-250 dye using starch/poly(alginic acid-cl-acrylamide) nanohydrogel, Process Saf. Environ. Protect. 109 (2017) 301–310, https://doi.org/10.1016/j.psep.2017.04.011.
[74] S. Gamoudi, E. Srasra, Adsorption of organic dyes by HDPy+-modified clay: effect of molecular structure on the adsorption, J. Mol. Struct. 1193 (2019) 522–531, https://doi.org/10.1016/j.molstruc.2019.05.055.

[75] A.H. Berger, A.S. Bhown, Comparing physisorption and chemisorption solid sorbents for use separating CO2 from flue gas using temperature swing adsorption, Energy Proc. 4 (2011) 562–567, https://doi.org/10.1016/j.egypro.2011.01.089.
[76] A.B.D. Nandiyanto, S.-G. Kim, F. Iskandar, K. Okuyama, Synthesis of spherical mesoporous silica nanoparticles with nanometer-size controllable pores and outer diameters, Microporous Mesoporous Mater. 120 (3) (2009) 447–453, https://doi.org/10.1016/j.micromeso.2008.12.019.
[77] S. Lahreche, I. Moulefera, A. El Kebir, L. Sabantina, A.(Benyoucef, Application of activated carbon adsorbents prepared from prickly pear fruit seeds and a conductive polymer matrix to remove Congo red from aqueous solutions, Fibers 10 (1) (2022) 7, https://doi.org/10.3390/fib10010007.
[78] D. Kołodyńska, E. Skwarek, Z. Hubicki, W. Janusz, Effect of adsorption of Pb(II) and Cd(II) ions in the presence of EDTA on the characteristics of electrical double layers at the ion exchanger/NaCl electrolyte solution interface, J. Colloid Interface Sci. 333 (2) (2009) 448–456, https://doi.org/10.1016/j.jcis.2009.02.002.
[79] K. Naseem, R. Begum, W. Wu, M. Usman, A. Irfan, A.G. Al-Sehemi, Z.H. Farooqi, Adsorptive removal of heavy metal ions using polystyrene-poly(N-isopropylmethacrylamide-acrylic acid) core/shell gel particles: adsorption isotherms and kinetic study, J. Mol. Liq. 277 (2019) 522–531, https://doi.org/10.1016/j.molliq.2018.12.054.